Geophysical Research Letters

RESEARCH LETTER
10.1029/2022GL102074

Equatorial Undercurrent Influence on Surface Seawater $\delta^{18}O$ Values in the Galápagos

Jessica L. Conroy[1,2], Nicole K. Murray[1], Gillian S. Patterson[3], Aiden I. G. Schore[2], Ima Ikuru[1], Julia E. Cole[4], David Chillagana[5], and Fernando Echeverria[5]

[1]Department of Geology, The University of Illinois at Urbana-Champaign, Urbana, IL, USA, [2]Department of Plant Biology, The University of Illinois at Urbana-Champaign, Urbana, IL, USA, [3]Department of Physics, The University of Illinois at Urbana-Champaign, Urbana, IL, USA, [4]Department of Earth and Environmental Sciences, University of Michigan, Ann Arbor, MI, USA, [5]Charles Darwin Research Foundation, Puerto Ayora, Ecuador

Key Points:

- Galápagos seawater $\delta^{18}O$ values strongly covary with equatorial cold tongue salinity values
- Seawater $\delta^{18}O$ values are higher with a stronger Pacific Equatorial Undercurrent west of Galápagos

Supporting Information:

Supporting Information may be found in the online version of this article.

Correspondence to:

J. L. Conroy,
jconro@illinois.edu

Citation:

Conroy, J. L., Murray, N. K., Patterson, G. S., Schore, A. I. G., Ikuru, I., Cole, J. E., et al. (2023). Equatorial Undercurrent influence on surface seawater $\delta^{18}O$ values in the Galápagos. *Geophysical Research Letters*, *50*, e2022GL102074. https://doi.org/10.1029/2022GL102074

Received 16 NOV 2022
Accepted 24 JAN 2023

Author Contributions:

Conceptualization: Jessica L. Conroy
Data curation: Jessica L. Conroy
Formal analysis: Jessica L. Conroy, Nicole K. Murray, Gillian S. Patterson, Aiden I. G. Schore, Ima Ikuru
Funding acquisition: Jessica L. Conroy
Investigation: Jessica L. Conroy, Nicole K. Murray, Gillian S. Patterson, Aiden I. G. Schore, Ima Ikuru, Julia E. Cole
Methodology: Jessica L. Conroy, David Chillagana, Fernando Echeverria
Project Administration: Jessica L. Conroy
Resources: Jessica L. Conroy, David Chillagana, Fernando Echeverria
Software: Jessica L. Conroy
Supervision: Jessica L. Conroy
Validation: Jessica L. Conroy
Visualization: Jessica L. Conroy
Writing – original draft: Jessica L. Conroy

Abstract Stable isotopes of oxygen ($\delta^{18}O$) in seawater reflect the combined influences of ocean circulation and atmospheric moisture balance. However, it is difficult to disentangle disparate ocean and atmosphere influences on modern seawater $\delta^{18}O$ values, partly because continuous time series of seawater $\delta^{18}O$ are rare. Here we present a nearly nine-year, continuous record of seawater $\delta^{18}O$ values from the Galápagos. Seawater $\delta^{18}O$ values faithfully track sea surface salinity and salinity along the equator at 50 m depth. Zonal current velocity within the Equatorial Undercurrent (EUC), directly west of the Galápagos, is strongly correlated with Galápagos surface seawater $\delta^{18}O$ values with a 1-month lag. Reconstructions of Galápagos seawater $\delta^{18}O$ values could thus provide a window into past variations in the strength of the EUC, an important influence on large-scale tropical Pacific climate.

Plain Language Summary The Equatorial Undercurrent (EUC) flows beneath the surface of the equatorial Pacific Ocean from west to east, transporting cold, salty, nutrient rich waters. When this current hits the Galápagos, it rises to the surface. Its high nutrient levels serve as the foundation for the diverse Galápagos ecosystem and its colder temperature helps set up a strong sea surface temperature gradient that is the foundation of the tropical Pacific climate system. Despite its importance, little is known about how this current has varied prior to the short period of instrumental observations, and it remains challenging to reproduce in climate models. Here we show how Galápagos seawater stable isotope values track the strength of the EUC. Our findings open up possibilities to extend the record of the EUC back in time with isotope-based paleoclimate proxies from the Galápagos region.

1. Introduction

Stable oxygen isotopes in seawater have a long history of utility in defining large-scale water masses and water mass mixing, sea ice melt, and continental runoff to the ocean (i.e., Akhoudas et al., 2021; Biddle et al., 2019; Frew et al., 2000; LeGrande & Schmidt, 2006; Reyes-Macaya et al., 2022; Schlosser et al., 2002). Seawater $\delta^{18}O$ (hereafter $\delta^{18}O_{sw}$) values also preserve information about precipitation and evaporation over the ocean, which assert a large control on mixed layer $\delta^{18}O_{sw}$ values. As such, $\delta^{18}O_{sw}$ values have a strong, linear relationship with salinity, given that freshwater fluxes influence both variables in a similar manner (Conroy et al., 2017; Reed et al., 2022; Thompson et al., 2022). However, $\delta^{18}O_{sw}$ values reflect more than salinity, as precipitation $\delta^{18}O$ values vary spatially and temporally, and because atmospheric conditions alter the degree of isotope fractionation during evaporation (Craig & Gordon, 1965). Moreover, advection and upwelling transport waters with varying $\delta^{18}O_{sw}$ values, complicating interpretation of $\delta^{18}O_{sw}$ as a simple hydroclimatic indicator in some regions of the ocean.

$\delta^{18}O_{sw}$ information can be extracted from the measured $\delta^{18}O$ values of marine carbonate climate archives, such as fossil coral skeletons and foraminifera tests. However, in these materials, carbonate $\delta^{18}O$ values also vary with temperature, given the temperature-dependence of equilibrium stable isotope fractionation. If the temperature component can be isolated, such as with paired measurements of the temperature proxy Sr/Ca in corals (McCulloch et al., 1994; Walter et al., 2022), past $\delta^{18}O_{sw}$ values can be calculated and used to interpret past salinity, hydroclimate, and ocean dynamics. In some regions, where $\delta^{18}O_{sw}$ controls a larger portion of carbonate

Writing – review & editing: Jessica L. Conroy, Julia E. Cole, David Chillagana, Fernando Echeverria

$\delta^{18}O$ variance, $\delta^{18}O_{sw}$ and salinity can also be directly inferred from carbonate $\delta^{18}O$ measurements (Thompson et al., 2022).

A key challenge in such efforts is the limited understanding of how $\delta^{18}O_{sw}$ values vary temporally. The majority of modern $\delta^{18}O_{sw}$ measurements come from sporadic, geographically limited research cruises. The resulting $\delta^{18}O_{sw}$ data from the last several decades has provided a useful temporal average of spatial $\delta^{18}O_{sw}$ variability across the global ocean (Figure 1a), but typically cannot define even seasonal $\delta^{18}O_{sw}$ variability. Few continuous time series of $\delta^{18}O_{sw}$ from single locations exist, given the challenges in maintaining such seawater collections over long periods of time (Conroy et al., 2017; DeLong et al., 2022). Thus, we still have little idea of how $\delta^{18}O_{sw}$ varies seasonally and interannually, with our current understanding coming mainly from isotope-enabled ocean model simulations. Models have revealed substantial temporal variability in both $\delta^{18}O_{sw}$ and the $\delta^{18}O_{sw}$-salinity relationship and the varied influence of atmospheric moisture balance, advection, vertical mixing, and diffusion on these values (Stevenson et al., 2018).

Here we present a 9-year, weekly-resolved record of $\delta^{18}O_{sw}$ from the Galápagos Archipelago in the eastern equatorial Pacific (Figure 1a). The Galápagos are located in a region with complex ocean circulation and strong interannual variability in atmospheric moisture balance due to the El Niño-Southern Oscillation (ENSO). Numerous $\delta^{18}O$-based paleoceanographic records from fossil corals and foraminifera have been developed here, which hold critical information on past changes in climate (Dunbar et al., 1994; Koutavas et al., 2006; Lea et al., 2000; Rustic et al., 2015; Shen et al., 1992). Previous research has revealed a relatively weak imprint of atmospheric moisture balance on Galápagos $\delta^{18}O_{sw}$ (Conroy et al., 2017; Russon et al., 2013; Stevenson et al., 2018; Wellington et al., 1996). Here we more comprehensively assess temporal variability in Galápagos $\delta^{18}O_{sw}$ values and potential atmospheric and oceanic drivers of this temporal variability using one of the longest available $\delta^{18}O_{sw}$ time series to date.

2. Study Site and Methods

2.1. Study Site

Galápagos, Ecuador, situated along the equator in the eastern tropical Pacific Ocean (Figure 1a), is under the influence of large-scale atmospheric subsidence and the southeasterly trade winds associated with the zonal Pacific Walker Circulation. The islands are also positioned within the 'cold tongue' of cooler mean sea surface temperatures (SST) in the eastern to central equatorial Pacific. Galápagos climate is arid at sea level, but higher relative humidity and precipitation rates occur at the higher island elevations. The Galápagos seasonal cycle consists of a warm-wet season from December to May and a cool-dry season from June to November (Trueman & d'Ozouville, 2010). Although the Galápagos are consistently south of the Intertropical Convergence Zone (ITCZ), the southward shift of the ITCZ in boreal winter leads to weaker trade winds, reduced upwelling, warmer SST and air temperatures, and enhanced precipitation.

Interannual climate variability associated with ENSO is prominent in the Galápagos. La Niña periods have stronger trade winds and upwelling, cooler SST, and little to no precipitation at sea level in the Galápagos. During El Niño events, weakened trade winds, a deeper thermocline, and warm SST lead to increased precipitation that can be an order of magnitude higher than average (Martin et al., 2018). These conditions are especially pronounced during eastern Pacific - style El Niño events (e.g., Capotondi et al., 2015).

Ocean circulation in and around the Galápagos archipelago is complex, with multiple ocean currents converging in the region (Kessler, 2006; Liu et al., 2014). At the surface, the westward South Equatorial Current (SEC) flows across the northern and southern boundaries of the Galápagos platform. The southwestward Panama Current strongly influences the surface waters of the northeastern archipelago, carrying relatively warm and low salinity waters into the area. The northwestward Peru Coastal Current, or Humboldt Current, transports cooler, upwelled, nutrient-rich waters toward the islands and feeds the southern lobe of the SEC. The relatively cool and saline Equatorial Undercurrent (EUC), or Cromwell Current, flowing from west to east 50–100 m below the sea surface between 1°N and 2°S, intersects the Galápagos and shoals along the western shores of the westernmost islands of Fernandina and Isabela, leading to much cooler SST (Karnauskas et al., 2010). The EUC then splits into northern and southern branches around the islands (Jakoboski et al., 2020). These upwelled EUC waters are nutrient-rich, making the EUC a key influence on the Galápagos marine ecosystem (Palacios, 2004).

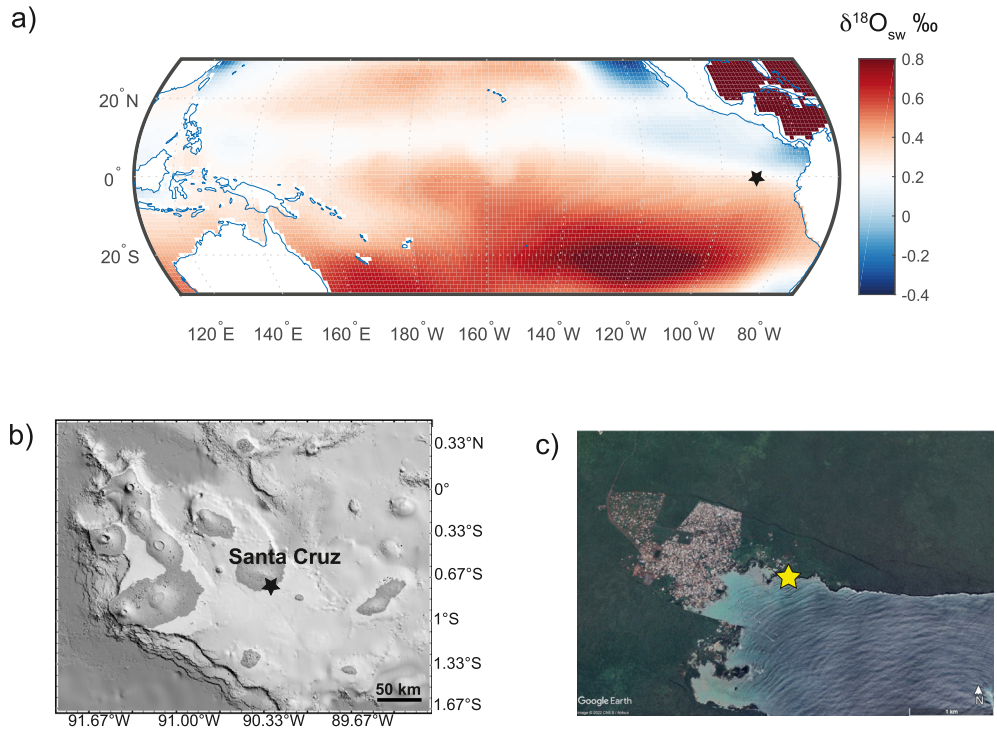

Figure 1. (a) Map of spatially interpolated mean $\delta^{18}O_{sw}$ of the tropical Pacific (LeGrande & Schmidt, 2006). Galápagos archipelago indicated by black star. (b) Topographic and bathymetric map of the Galápagos (modified from Martin et al., 2018) with sampling location on Santa Cruz indicated by black star. (c) Satellite image of Puerto Ayora, Santa Cruz and vicinity, with sampling site indicated by yellow star (Google Earth Pro, 2022).

The long-term seawater sampling site of this study is located on the southeastern shore of Santa Cruz Island (Figure 1c), where sampling began in October 2012 (Conroy et al., 2017). The current data set ends in May 2021 and is mostly continuous, apart from one hiatus from January to May 2018. Seawater samples were taken once a week at 6:00 a.m. at La Ratonera beach (0.7437°S, 90.3031°W), off a rocky area of the beach, where wave action is generally intense. Spatial seawater sampling in 2012 and 2015 indicated the $\delta^{18}O_{sw}$ and salinity values at this site were similar to seawater measured across the platform at the time of sampling (Conroy et al., 2017).

Along with seawater samples, precipitation samples for isotope analysis were collected daily from October 2012 through January 2021 at the Charles Darwin Research Station weather station located ~100 m from La Ratonera Beach. Samples were collected daily, on days with rain, in a separatory funnel containing mineral oil to hinder water evaporation. An additional seven samples of Santa Cruz groundwater from trips in 2012, 2015, and 2021 were measured for isotopic analysis (Table S1 in Supporting Information S1). These data are assessed along with four samples of previously published Santa Cruz groundwater stable isotope data from Warrier et al. (2012).

The main salinity and current datasets assessed with respect to the new Galápagos data are from the GLORYS12 Reanalysis from the Copernicus Marine Environment Monitoring Service (Jean-Michel et al., 2021). This eddy-resolving, 1/12° data set spans the majority of the sampling period, ending in May 2020. Other datasets analyzed include WHOI OAflux v3 evaporation rates over the ocean (Yu & Weller, 2007), PEODAS 20°C isotherm depth (Yin et al., 2011), ERA5 reanalysis sea level pressure (SLP, Hersbach et al., 2020), UK Met Office Hadley Centre EN4.2.2 salinity (Good et al., 2013), and the NCEP Global Ocean Data Assimilation System (GODAS) zonal and meridional currents (Behringer & Xue, 2004). Charles Darwin Research Station weather station precipitation data are also assessed, as is precipitation at the Bellavista, Santa Cruz, station at 191 masl. We also assessed daily and hourly sea level measurements taken at Puerto Ayora (Caldwell et al., 2015), and sea surface temperature measurements taken daily by station personnel at the seawater sampling site.

2.2. Sample Measurements

Precipitation and groundwater samples were stored in 3.5 ml crimp-top glass vials, and seawater and groundwater samples were stored in 60 mL amber bottles capped and sealed with parafilm. Samples from April 2016 onward were analyzed for both $\delta^{18}O$ and $\delta^{2}H$ at the University of Illinois at Urbana-Champaign on a Picarro L-2140i water isotope analyzer. Previous samples, reported in Conroy et al. (2017), were measured on a Picarro L-2130i water isotope analyzer. Samples were calibrated with three internal standards, which were in turn calibrated to Vienna Standard Mean Ocean Water 2 (VSMOW2), Greenland Ice Sheet Project (GISP) and Standard Light Antarctic Precipitation 2 (SLAP2) standards. We applied corrections as discussed in Van Geldern and Barth, (2012) to account for memory effects and instrument drift. Data are expressed in standard δ-notation. Total error is <0.1‰ for $\delta^{18}O$ and <0.8‰ for $\delta^{2}H$. Although $\delta^{2}H$ values are not discussed in this work, these additional values were used to identify and exclude samples affected by evaporation after collection (see results).

From October 2012–September 2020, seawater salinity was measured on a Thermo Scientific Orion Star A212 benchtop conductivity meter. The meter was calibrated every 10 samples with 50.0 mS/cm certified conductivity solution. Twenty mL samples were measured 5 times at a constant temperature of 25.0°C. Salinity values in PSU are reported as the average of the five measurements. Measured standard deviations for individual samples are <0.1 PSU and duplicate measurements on samples indicate a mean absolute difference of 0.1 PSU. From October 2020 onward, salinity was measured on a Guildline Autosal 8400B, using IAPSO standard seawater (34.994 PSU) as a daily standard. Total precision is < ± 0.002 PSU.

3. Results

A total of 417 seawater samples from October 2012 to May 2021 are analyzed, including data through April 2016 previously published in Conroy et al. (2017). The $\delta^{18}O_{sw}$ values range from −2.03 to 0.71‰, with a mean of 0.06 ± 0.36‰ (1s, used throughout). Salinity values range from 9.16 PSU to 35.51 PSU, with a mean of 32.05 ± 4.06 PSU (Figure S1 in Supporting Information S1).

Aperiodic freshwater pulses in the seawater time series are identified using salinity outliers, calculated as 1.5 times the interquartile range below the 25th percentile (Figure S2a in Supporting Information S1). With this method, salinity values <29 PSU are considered unrepresentative of open ocean salinity and $\delta^{18}O_{sw}$. NASA Aquarius v4 daily sea surface salinity measurements from 2011 to 2015 also reveal a minimum value of 29 PSU for the 0.5° × 0.5° grid cell that encompasses our sample site (Figure S2b in Supporting Information S1, Melnichenko et al., 2016). We identify 51 (12% of the data) of these freshwater pulses. They occur in every month of the year, with more pulses in March ($N = 8$) and December ($N = 6$) (Figure S3 in Supporting Information S1). These pulses are discussed further in the supporting online material, but are excluded from monthly averaged $\delta^{18}O_{sw}$ values and subsequent analyses that aim to consider the drivers of $\delta^{18}O_{sw}$ values more representative of the open ocean.

Monthly averaged $\delta^{18}O_{sw}$ values, excluding freshwater pulses, range from −0.18 to 0.44‰, with a mean of 0.16 ± 0.13‰. Salinity values range from 30.81 PSU to 35.15 PSU, with a mean of 33.34 ± 0.88 PSU Monthly average $\delta^{18}O_{sw}$ and salinity show that high salinity and $\delta^{18}O_{sw}$ values occur from May to August, with lower values from November to February (Figure S4 in Supporting Information S1). The linear fit of monthly $\delta^{18}O_{sw}$ and salinity values, excluding freshwater pulses, produces a slope of 0.13 ± 0.02‰/PSU and an intercept of −4.03 ± 0.49‰ ($R^2 = 0.74$). Temporal variability in the linear $\delta^{18}O_{sw}$—salinity relationship is discussed further in the supporting online material.

610 precipitation samples from October 2012 to March 2021, which include previously published data through 27 March 2016 in Martin et al. (2018) are also reported here (Figure S5 in Supporting Information S1). Outliers that represent evaporated samples were identified using calculated d-excess values ($\delta^{2}H$-8*$\delta^{18}O$). Ten samples were excluded from analysis as their d-excess values were lower than 3 sigma below the median precipitation d-excess value (d-excess<1.44‰). The meteoric water line slope (6.75 ± 0.18) and intercept (d-excess value, 7.67 ± 0.25) for this longer data set are slightly higher than those reported in Martin et al. (2018). Precipitation $\delta^{18}O$ values range from −5.57 to 1.09‰ (mean −1.10 ± 0.88‰). Monthly, amount-weighted averages ($N = 94$) show a seasonal cycle, with lower $\delta^{18}O$ values from February to June (−1.33‰ to −2.95‰), when precipitation rates are higher, and higher $\delta^{18}O$ values from July to January (−0.65‰ to −1.05‰), when precipitation rates are lower (Figure S5b in Supporting Information S1).

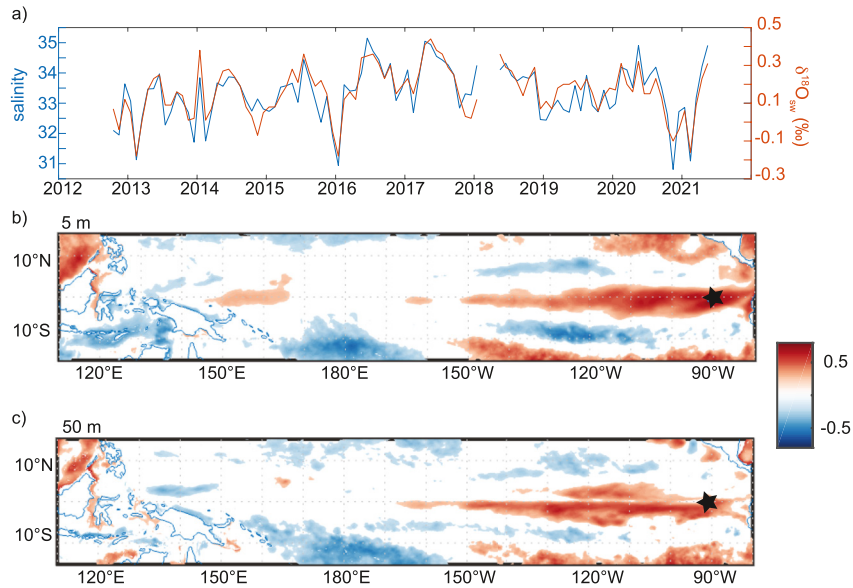

Figure 2. (a) Monthly Galápagos $\delta^{18}O_{sw}$ and salinity values. (b) Correlation map of monthly $\delta^{18}O_{sw}$ and GLORYS12 salinity at 5 m depth across the tropical Pacific. (c) Correlation map of monthly $\delta^{18}O_{sw}$ and GLORYS12 salinity at 50 m depth across the tropical Pacific. Only values significant at the 95% confidence interval are plotted. Galápagos indicated by black star.

Mean groundwater $\delta^{18}O$ and $\delta^{2}H$ values are $-2.33 \pm 0.48‰$ and $-8.16 \pm 2.44‰$, respectively. Values decrease at higher elevations, with the lowest values from samples taken at Santa Rosa (500 masl) by Warrier et al. (2012) and the highest values in Puerto Ayora groundwater (Table S1 in Supporting Information S1). The groundwater $\delta^{18}O$ and $\delta^{2}H$ values fall on the precipitation meteoric water line (Figure S5a in Supporting Information S1).

4. Discussion

4.1. Salinity and Atmospheric Controls on $\delta^{18}O_{sw}$ Values

Galápagos $\delta^{18}O_{sw}$ is highly correlated not only with measured salinity on the paired water samples (Table S2 in Supporting Information S1, Figure 2a), but with GLORYS12 reanalysis salinity values across the surface eastern-central equatorial cold tongue region (5 m depth) and in the subsurface at 50 m depth (Figures 2b and 2c). We also observe similar correlation patterns using the EN4.2.2 objective analysis salinity product from October 2012 to May 2021 (e.g., extending a year beyond GLORYS12 reanalysis, Figure S6 in Supporting Information S1). Thus, $\delta^{18}O_{sw}$ is a proxy for regional as well as local surface and sub-surface salinity variability.

Although $\delta^{18}O_{sw}$ and salinity are often interpreted in the context of hydroclimate, the influence of atmospheric moisture balance on Galápagos $\delta^{18}O_{sw}$ values is relatively weak (Figure S7, Table S2 in Supporting Information S1). Higher monthly precipitation and low monthly precipitation $\delta^{18}O$ at sea level (Puerto Ayora) do not lead to lower $\delta^{18}O_{sw}$ values. We also assessed $\delta^{18}O_{sw}$ relative to monthly precipitation measured at 191 masl, in the town of Bellavista. Precipitation $\delta^{18}O$ values are not only higher in the highlands but also decrease with elevation on Santa Cruz due to orographic rainout-related effects (Martin et al., 2018). However, the relationship between Bellavista precipitation and $\delta^{18}O_{sw}$ is not significant, up to a lag of 6 months (Table S3 in Supporting Information S1). We do find a significant, negative relationship between monthly Bellavista precipitation anomalies (after removing the long-term monthly means) and $\delta^{18}O_{sw}$ at a lag of 5 months (Table S3 in Supporting Information S1). This lagged relationship suggests that groundwater flow from the highlands and subsequent groundwater seepage following periods of higher precipitation rates may play a small role in reducing $\delta^{18}O_{sw}$ values, but overall, the influence of local precipitation on monthly $\delta^{18}O_{sw}$ values is weak. A significant, negative correlation is observed with regional ocean evaporation (Table S2 in Supporting Information S1). This direction of the relationship is opposite to the expected relationship (i.e., more evaporation will increase $\delta^{18}O_{sw}$). This suggests another unknown factor is likely influencing both evaporation and $\delta^{18}O_{sw}$.

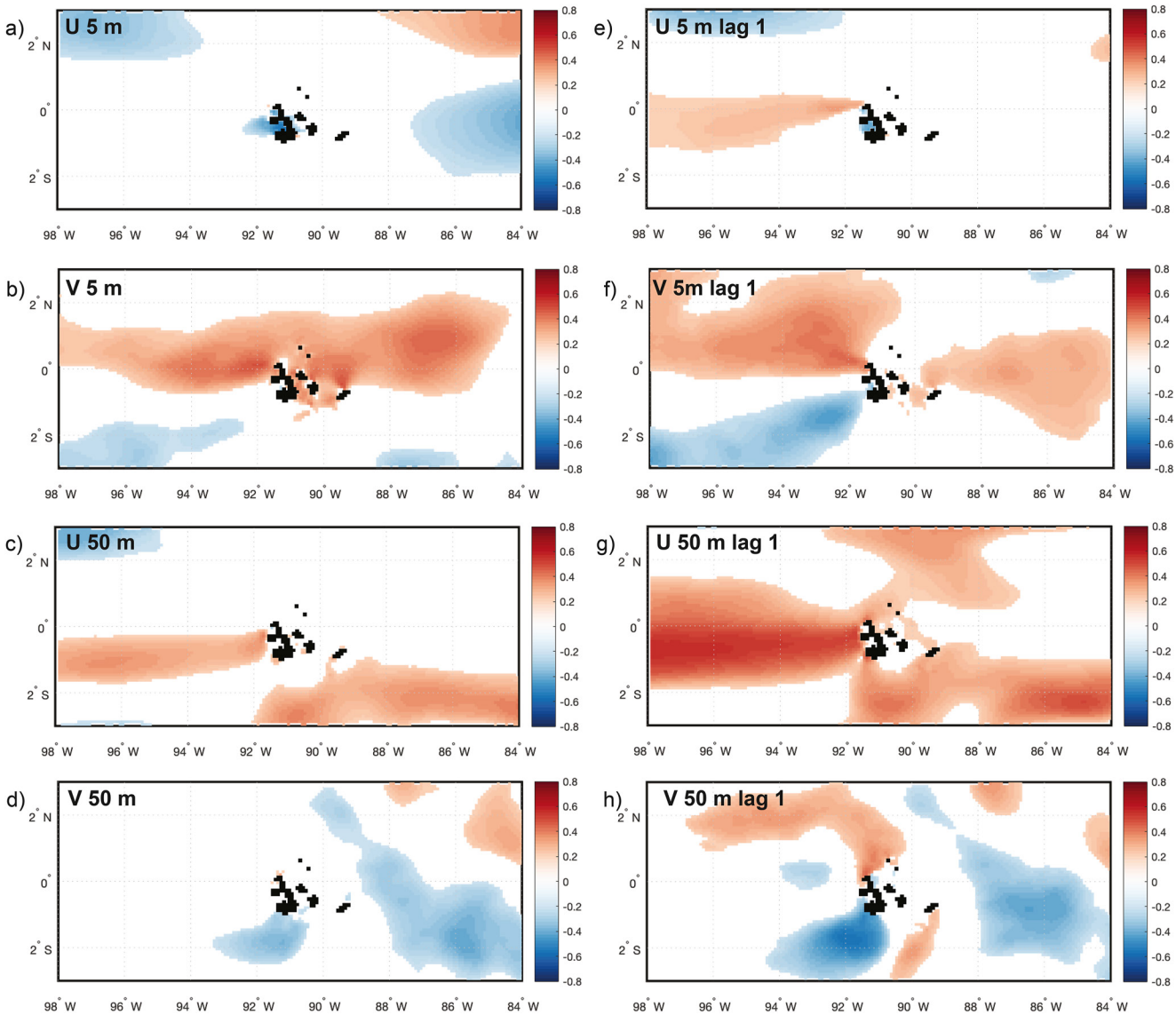

Figure 3. Map of correlation coefficients between regional GLORYS12 zonal (U) and meridional (V) current velocity and $\delta^{18}O_{sw}$ at (a, b) 5 m depth and (c, d) 50 m depth. (e–h) As in (a–d) but with $\delta^{18}O_{sw}$ lagging by 1 month.

4.2. Influence of Advection and the EUC on $\delta^{18}O_{sw}$ Values

The strong correlations between Galápagos $\delta^{18}O_{sw}$ and salinity on the equator at 50 m depth, west of the Galápagos, suggests that the higher salinity waters that covary with high $\delta^{18}O_{sw}$ waters near Santa Cruz may be transported to the site by the EUC. Along with high salinity, waters of the EUC also have relatively high $\delta^{18}O_{sw}$ values. In the central equatorial Pacific, mean EUC $\delta^{18}O_{sw}$ values range from 0.41 to 0.51‰ (Conroy et al., 2014). Closer to the Galápagos, data from the NASA GISS $\delta^{18}O_{sw}$ database reveal a mean $\delta^{18}O_{sw}$ value of 0.37 ± 0.09‰ from 5 measurements between 95° and 86°W, along the equator, between 50 and 100 m depth (Schmidt et al., 1999).

Along with salinity, an EUC signature in Galápagos $\delta^{18}O_{sw}$ should also be reflected in correlations with zonal current speed between 0 and 1°S just west of the Galápagos (Johnson et al., 2002; Karnauskas et al., 2010). At a depth of 50 m, west of the archipelago, which approximates the location of the EUC, we find strong, positive correlations between Galápagos $\delta^{18}O_{sw}$ values and zonal current speed when $\delta^{18}O_{sw}$ lags zonal current speed by 1 month (Figure 3). That is, higher Galápagos $\delta^{18}O_{sw}$ values coincide with stronger eastward current speed in the prior month (Figure 3). We also observe a strong, positive correlation with zonal current velocity with depth at 93°W, peaking at 0.67°S–0.75°, 47–55 m depth (Figure 4). Periods of higher $\delta^{18}O_{sw}$ coincide with

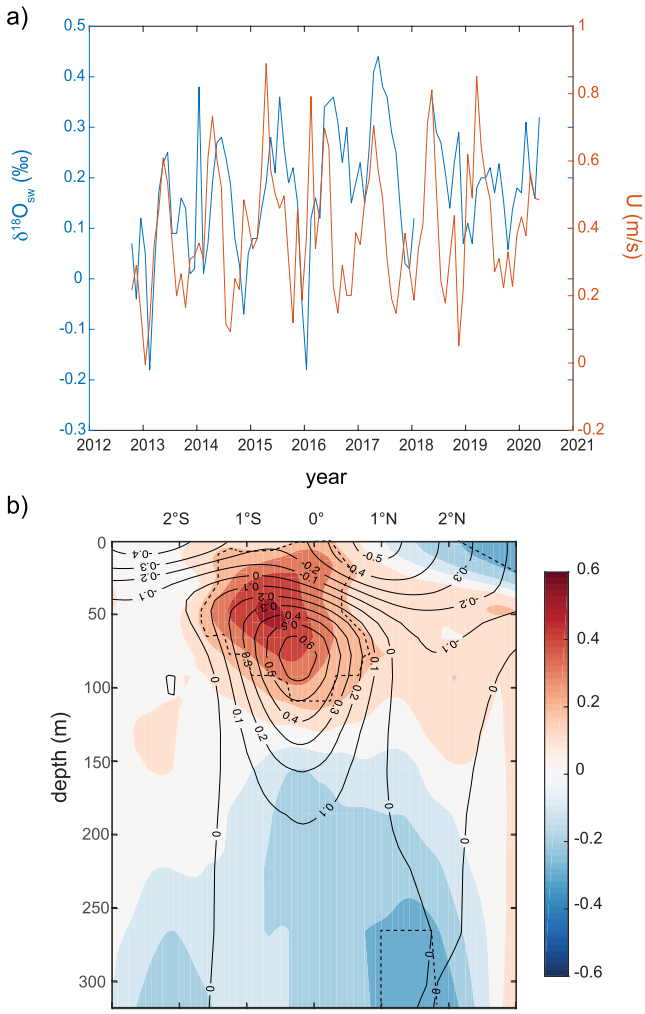

Figure 4. (a) Monthly $\delta^{18}O_{sw}$ and GLORYS12 zonal velocity averaged over 0.67°S–0.75°, 93°W, 47–55 m depth. (b) Correlation coefficients between monthly $\delta^{18}O_{sw}$ and GLORYS12 zonal velocity averaged over 93°W. One month lag applied to $\delta^{18}O_{sw}$ data. Dashed lines represent significant correlations at the 95% confidence level. Black contours represent the mean zonal current speed, 1993–2020.

higher eastward current velocity when $\delta^{18}O_{sw}$ lags zonal velocity by 1 month ($r = 0.52$, $p < 0.001$, $N = 92$). A similar relationship is found when using GODAS zonal velocity, which extends to May 2021 (Figure S8 in Supporting Information S1).

The structure of the correlations in Figure 4 reflects the structure of the EUC itself; however, correlations peak to the south and closer to the surface than the long-term mean zonal current speed (Figure 4b, black contours). This offset provides insight into the conditions that lead the EUC to imprint on Galápagos $\delta^{18}O_{sw}$ values. When the EUC is faster, closer to the surface and located slightly further south than normal, a greater proportion of EUC waters reaches the southern coast of Santa Cruz. In sum, higher monthly Galápagos $\delta^{18}O_{sw}$ values are due to a greater proportion of EUC waters in the mixed layer during periods of stronger, more southerly, and shallow EUC flow, and Galápagos $\delta^{18}O_{sw}$ values appear to be an excellent proxy for regional EUC strength.

It is still unclear how the EUC contributes to sources of upwelled waters on the Galápagos platform. The EUC shoals as it approaches the topographic barrier of the Galápagos, and bifurcates into a northern and southern current around the archipelago (Jakoboski et al., 2020). This bifurcation and shoaling is also reflected in the change in sign of the correlation coefficients between Galápagos $\delta^{18}O_{sw}$ and meridional current speed, both at 50 and 5 m depth (Figure 3). One high-resolution mean current analysis reveals both the southern and northern EUC branches may flow onto the eastern platform at 40–160 m depth (Karnauskas et al., 2010). High-resolution ocean modeling of surface flow in and around the Galápagos archipelago by Liu et al. (2014) also show surface eastward flow onto the Galápagos platform originating from the EUC to the west, in this case even reaching the southern Santa Cruz coast. The 1-month lag in the EUC-Galápagos $\delta^{18}O_{sw}$ relationships suggests a transit time of this order between the EUC just west of the archipelago and the measurement site on the coast of Santa Cruz. Higher EUC velocity has also been found to lead higher salinity by 30 days south of the equator around the Galápagos (Rudnick et al., 2021).

The relationship between the EUC and Galápagos $\delta^{18}O_{sw}$ is highly seasonal; When a 1-month lag is applied, the relationship between climatological mean monthly $\delta^{18}O_{sw}$ and the EUC is strong ($r = 0.77$, $p = 0.004$, $N = 12$). Zonal current speed at 93°W, 0.67°S-0.75°, 47–55 m depth, is highest from March through June in the time period analyzed, consistent with observations of an overall stronger EUC in the boreal spring. $\delta^{18}O_{sw}$ is highest in April through August (Figure S4 in Supporting Information S1). The one-month lagged correlation between $\delta^{18}O_{sw}$ and the EUC timeseries at 93°W is also retained (although weaker) with the removal of the long-term monthly mean values from each time series, indicating that this relationship is interannual as well as seasonal ($r = 0.30$, $p = 0.006$, $N = 91$, Figure S9a in Supporting Information S1). Overall, the EUC is observed to be weaker during El Niño events, although at 93°W, it is not highly correlated with surface temperature anomalies (Johnson et al., 2002; Rudnick et al., 2021). During La Niña periods, as indicated by NIÑO1+2 Index values <0°C, the relationship between anomalies of $\delta^{18}O_{sw}$ and the 93°W EUC timeseries is stronger (Figure S9b in Supporting Information S1).

5. Conclusions and Implications

Many paleoceanographic records from the Galápagos have been developed from fossil coral and foraminifera $\delta^{18}O$ values over the last three decades (Dunbar et al., 1994; Koutavas et al., 2006; Lea et al., 2000; Rustic et al., 2015; Shen et al., 1992). These records are a mixed contribution of $\delta^{18}O_{sw}$ values and temperature, with evaluations to date showing the dominance of temperature on coral carbonate $\delta^{18}O$ values in this region

(Thompson et al., 2022). However, more recent work pairing foraminifera Mg/Ca and $\delta^{18}O$ measurements and coral Sr/Ca and $\delta^{18}O$ measurements from around the archipelago offer the potential for future $\delta^{18}O_{sw}$ and salinity reconstructions (Cheung et al., 2021; Jimenez et al., 2018; Rustic et al., 2015). Our work provides an important new context for interpreting such data. Although atmospheric moisture balance is the common focus of $\delta^{18}O_{sw}$ interpretations (Thompson et al., 2022; Walter et al., 2022), our findings show stronger potential for Galápagos $\delta^{18}O_{sw}$ values to be used to reconstruct the strength of the EUC. Such a reconstruction would be novel and useful, given the critical role of the EUC in supporting the zonal gradient of sea surface temperature across the tropical Pacific and contributing to regional productivity. The EUC has also gained considerable importance as a climate model diagnostic, as it is not always well-simulated, with cascading implications for the tropical Pacific climate system (Karnauskas et al., 2020). Ultimately then, this work suggests Galápagos paleo-$\delta^{18}O_{sw}$ reconstructions could be developed to benchmark the EUC in paleoclimate model simulations.

Data Availability Statement

$\delta^{18}O_{sw}$ and salinity data are archived on the Seawater Oxygen Isotope Community Database (Conroy, 2023). Precipitation and groundwater isotope data are available through the Water Isotopes Database (https://wateriso.utah.edu/waterisotopes/pages/spatial_db/SPATIAL_DB.html).

Acknowledgments
This work is funded by NSF-CA-REER-1847791to JLC. We are grateful to the Charles Darwin Research Station for their logistic support and the Galápagos National Park for the scientific permits to conduct this research. This publication is contribution number 2482 of the Charles Darwin Foundation for the Galápagos Islands.

References

Akhoudas, C. H., Akhoudas, C. H., Akhoudas, C. H., Meredith, M. P., Garabato, A. N., Reverdin, G., et al. (2021). Ventilation of the abyss in the Atlantic sector of the southern ocean. *Scientific Reports*, *11*(1), 6760. https://doi.org/10.1038/s41598-021-86043-2

Behringer, D. W., & Xue, Y. (2004). Evaulation of the global ocean data assimilation system at NCEP: The Pacific Ocean. In *Eighth symposium on integrated observing and assimilation systems for atmosphere, oceans, and land surface, AMS 84th annual meeting*.

Biddle, L. C., Loose, B., & Heywood, K. J. (2019). Upper ocean distribution of glacial meltwater in the Amundsen Sea, Antarctica. *Journal of Geophysical Research: Oceans*, *124*(10), 6854–6870. https://doi.org/10.1029/2019jc015133

Caldwell, P. C., Merrifield, M. A., & Thompson, P. R. (2015). Sea level measured by tide gauges from global oceans—The joint archive for sea level holdings (NCEI accession 0019568), version 5.5. Dataset. *NOAA National Centers for Environmental Information*. https://doi.org/10.7289/V5V40S7W

Capotondi, A., Wittenberg, A. T., Newman, M., Di Lorenzo, E., Yu, J.-Y., Braconnot, P., et al. (2015). Understanding ENSO diversity. *Bulletin of the American Meteorological Society*, *96*(6), 921–938. https://doi.org/10.1175/bams-d-13-00117.1

Cheung, A. H., Cole, J. E., Thompson, D. M., Vetter, L., Jimenez, G., & Tudhope, A. W. (2021). Fidelity of the coral Sr/Ca paleothermometer following heat stress in the northern Galápagos. *Paleoceanography and Paleoclimatology*, *36*(12), e2021PA004323. https://doi.org/10.1029/2021PA004323

Conroy, J. L. (2023). Galápagos temporal seawater isotope and salinity data, version 1.0. *Interdisciplinary Earth Data Alliance (IEDA)*. https://doi.org/10.26022/IEDA/112750

Conroy, J. L., Cobb, K. M., Lynch-Stieglitz, J., & Polissar, P. J. (2014). Constraints on the salinity–oxygen isotope relationship in the central tropical Pacific Ocean. *Marine Chemistry*, *161*, 26–33. https://doi.org/10.1016/j.marchem.2014.02.001

Conroy, J. L., Thompson, D. M., Cobb, K. M., Noone, D., Rea, S., & Legrande, A. N. (2017). Spatiotemporal variability in the $\delta^{18}O$-salinity relationship of seawater across the tropical Pacific Ocean. *Paleoceanography*, *32*(5), 484–497. https://doi.org/10.1002/2016PA003073

Craig, H., & Gordon, L. I. (1965). Deuterium and oxygen 18 variations in the ocean and the marine environment. In E. Tongiorgi (Ed.), *Stable isotopes in oceanographic studies and paleotempertures*, *Consiglio nazionale delle richerche* (pp. 9–130).

DeLong, K. L., Atwood, A., Moore, A., & Sanchez, S. (2022). Clues from the sea paint a picture of Earth's water cycle. *Eos*, *103*. https://doi.org/10.1029/2022EO220231

Dunbar, R. B., Wellington, G. M., Colgan, M. W., & Glynn, P. W. (1994). Eastern Pacific SST since 1600 AD the $\delta^{18}O$ record of climate variability in Galápagos corals. *Paleoceanography*, *9*(2), 291–315. https://doi.org/10.1029/93pa03501

Frew, R. D., Dennis, P. F., Heywood, K. J., Meredith, M. P., & Boswell, S. M. (2000). The oxygen isotope composition of water masses in the northern North Atlantic. *Deep Sea Research Part I: Oceanographic Research Papers*, *47*(12), 2265–2286. https://doi.org/10.1016/s0967-0637(00)00023-6

Good, S. A., Martin, M. J., & Rayner, N. A. (2013). EN4: Quality controlled ocean temperature and salinity profiles and monthly objective analyses with uncertainty estimates. *Journal of Geophysical Research: Oceans*, *118*(12), 6704–6716. https://doi.org/10.1002/2013jc009067

Google Earth Pro. (2022). "Santa Cruz, Galápagos" version 7.3.4.8642.

Hersbach, H., Bell, B., Berrisford, P., Hirahara, S., Horányi, A., Muñoz-Sabater, J., et al. (2020). The ERA5 global reanalysis. *Quarterly Journal of the Royal Meteorological Society*, *146*(730), 1999–2049. https://doi.org/10.1002/qj.3803

Jakoboski, J., Todd, R. E., Owens, W. B., Karnauskas, K. B., & Rudnick, D. L. (2020). Bifurcation and upwelling of the equatorial Undercurrent west of the Galápagos archipelago. *Journal of Physical Oceanography*, *50*(4), 887–905. https://doi.org/10.1175/jpo-d-19-0110.1

Jean-Michel, L., Eric, G., Romain, B. B., Gilles, G., Angelique, M., Marie, D., et al. (2021). The Copernicus global 1/12° oceanic and sea ice GLORYS12 reanalysis. *Frontiers of Earth Science*, *9*. https://doi.org/10.3389/feart.2021.698876

Jimenez, G., Cole, J. E., Thompson, D. M., & Tudhope, A. W. (2018). Northern Galápagos corals reveal twentieth century warming in the eastern tropical Pacific. *Geophysical Research Letters*, *45*(4), 1981–1988. https://doi.org/10.1002/2017GL075323

Johnson, G. C., Sloyan, B. M., Kessler, W. S., & McTaggart, K. E. (2002). Direct measurements of upper ocean currents and water properties across the tropical Pacific during the 1990s. *Progress in Oceanography*, *52*(1), 31–61. https://doi.org/10.1016/s0079-6611(02)00021-6

Karnauskas, K. B., Jakoboski, J., Johnston, T. M. S., Owens, W. B., Rudnick, D. L., & Todd, R. E. (2020). The Pacific equatorial undercurrent in three generations of global climate models and glider observations. *Journal of Geophysical Research: Oceans*, *125*(11), e2020JC016609. https://doi.org/10.1029/2020JC016609

Karnauskas, K. B., Murtugudde, R., & Busalacchi, A. J. (2010). Observing the Galápagos–EUC interaction: Insights and challenges. *Journal of Physical Oceanography*, *40*(12), 2768–2777. https://doi.org/10.1175/2010jpo4461.1

Kessler, W. S. (2006). The circulation of the eastern tropical Pacific: A review. *Progress in Oceanography*, *69*(2–4), 181–217. https://doi.org/10.1016/j.pocean.2006.03.009

Koutavas, A., DeMenocal, P. B., Olive, G. C., & Lynch-Stieglitz, J. (2006). Mid-Holocene El Niño-Southern Oscillation (ENSO) attenuation revealed by individual foraminifera in eastern tropical Pacific sediments. *Geology*, *34*(12), 993–996. https://doi.org/10.1130/g22810a.1

Lea, D. W., Pak, D. K., & Spero, H. J. (2000). Climate impact of late quaternary equatorial Pacific Sea surface temperature variations. *Science*, *289*(5485), 1719–1724. https://doi.org/10.1126/science.289.5485.1719

LeGrande, A. N., & Schmidt, G. A. (2006). Global gridded data set of the oxygen isotopic composition in seawater. *Geophysical Research Letters*, *33*(12), L12604. https://doi.org/10.1029/2006GL026011

Liu, Y., Xie, L., Morrison, J. M., Kamykowski, D., & Sweet, W. V. (2014). Ocean circulation and water mass characteristics around the Galápagos Archipelago simulated by a multiscale nested ocean circulation model. *International Journal of Oceanography*, *2014*, 1–16. https://doi.org/10.1155/2014/198686

Martin, N. J., Conroy, J. L., Noone, D., Cobb, K. M., Konecky, B. L., & Rea, S. (2018). Seasonal and ENSO influences on the stable isotopic composition of Galápagos precipitation. *Journal of Geophysical Research: Atmospheres*, *123*(1), 261–275. https://doi.org/10.1002/2017JD027380

McCulloch, M. T., Gagan, M. K., Mortimer, G. E., Chivas, A. R., & Isdale, P. J. (1994). A high-resolution Sr/Ca and $\delta^{18}O$ coral record from the great barrier reef, Australia, and the 1982–1983 El Niño. *Geochimica et Cosmochimica Acta*, *58*(12), 2747–2754. https://doi.org/10.1016/0016-7037(94)90142-2

Melnichenko, D. O. (2016). *IPRC/SOEST Aquarius V4.0 Optimally Interpolated Sea Surface Salinity 7-Day global Dataset. Ver. 4.0*. PO.DAAC, CA, USA. https://doi.org/10.5067/AQR40-4U7CS

Palacios, D. M. (2004). Seasonal patterns of sea-surface temperature and ocean color around the galapagos: Regional and local influences. *Deep Sea Research Part II: Topical Studies in Oceanography*, *51*(1–3), 43–57. https://doi.org/10.1016/j.dsr2.2003.08.001

Reed, E. V., Thompson, D. M., & Anchukaitis, K. J. (2022). Coral-based sea surface salinity reconstructions and the role of observational uncertainties in inferred variability and trends. *Paleoceanography and Paleoclimatology*, *37*(6), e2021PA004371. https://doi.org/10.1029/2021PA004371

Reyes-Macaya, D., Hoogakker, B., Martinez-Mendez, G., Llanillo, P. J., Grasse, P., Mohtadi, M., et al. (2022). Isotopic characterization of water masses in the southeast Pacific region: Paleoceanographic implications. *Journal of Geophysical Research: Oceans*, *127*(1), e2021JC017525. https://doi.org/10.1029/2021JC017525

Rudnick, D. L., Owens, W. B., Johnston, T. S., Karnauskas, K. B., Jakoboski, J., & Todd, R. E. (2021). The equatorial current system west of the Galápagos islands during the 2014–16 El Niño as observed by underwater gliders. *Journal of Physical Oceanography*, *51*(1), 3–17. https://doi.org/10.1175/jpo-d-20-0064.1

Russon, T., Tudhope, A., Hegerl, G., Collins, M., & Tindall, J. (2013). Inter-annual tropical Pacific climate variability in an isotope-enabled CGCM: Implications for interpreting coral stable oxygen isotope records of ENSO. *Climate of the Past*, *9*(4), 1543–1557. https://doi.org/10.5194/cp-9-1543-2013

Rustic, G. T., Koutavas, A., Marchitto, T. M., & Linsley, B. K. (2015). Dynamical excitation of the tropical Pacific ocean and ENSO variability by little ice age cooling. *Science*, *350*(6267), 1537–1541. https://doi.org/10.1126/science.aac9937

Schlosser, P., Newton, R., Ekwurzel, B., Khatiwala, S., Mortlock, R., & Fairbanks, R. (2002). Decrease of river runoff in the upper waters of the Eurasian basin, Arctic ocean, between 1991 and 1996: Evidence from $\delta^{18}O$ data. *Geophysical Research Letters*, *29*(9), 3-1–3-4. https://doi.org/10.1029/2001gl013135

Schmidt, G. A., Bigg, G. R., & Rohling, E. J. (1999). Global seawater oxygen-18 database. Retrieved from http://data.giss.nasa.gov/o18data/

Shen, G. T., Cole, J. E., Lea, D. W., Linn, L. J., McConnaughey, T. A., & Fairbanks, R. G. (1992). Surface ocean variability at Galapagos from 1936–1982: Calibration of geochemical tracers in corals. *Paleoceanography*, *7*(5), 563–588. https://doi.org/10.1029/92pa01825

Stevenson, S., Powell, B. S., Cobb, K. M., Nusbaumer, J., Merrifield, M. A., & Noone, D. (2018). 20th century seawater $\delta^{18}O$ Dynamics and implications for coral-based climate reconstruction. *Paleoceanography and Paleoclimatology*, *33*(6), 606–625. https://doi.org/10.1029/2017PA003304

Thompson, D. M., Conroy, J. L., Konecky, B. L., Stevenson, S., DeLong, K. L., McKay, N., et al. (2022). Identifying hydro-sensitive coral delta O-18 records for improved high-resolution temperature and salinity reconstructions. *Geophysical Research Letters*, *49*(9), e2021GL096153. https://doi.org/10.1029/2021gl096153

Trueman, M., & d'Ozouville, N. (2010). Characterizing the Galápagos terrestrial climate in the face of global climate change. *Galápagos Research*, *67*, 26–37.

van Geldern, R., & Barth, J. A. C. (2012). Optimization of instrument setup and post-run corrections for oxygen and hydrogen stable isotope measurements of water by isotope ratio infrared spectroscopy (IRIS). *Limnology and Oceanography: Methods*, *10*(12), 1024–1036. https://doi.org/10.4319/lom.2012.10.1024

Walter, R. M., Sayani, H. R., Felis, T., Cobb, K. M., Abram, N. J., Arzey, A. K., et al. (2022). The CoralHydro2k database: A global, actively curated compilation of coral $\delta^{18}O$ and Sr/Ca proxy records of tropical ocean hydrology and temperature for the common era. *Earth System Science Data Discussions*, 1–56.

Warrier, R. B., Castro, M. C., & Hall, C. M. (2012). Recharge and source-water insights from the Galapagos Islands using noble gases and stable isotopes. *Water Resources Research*, *48*(3), W03508. https://doi.org/10.1029/2011wr010954

Wellington, G. M., Dunbar, R. B., & Merlen, G. (1996). Calibration of stable oxygen isotope signatures in Galapagos corals. *Paleoceanography*, *11*(4), 467–480. https://doi.org/10.1029/96pa01023

Yin, Y., Alves, O., & Oke, P. R. (2011). An ensemble ocean data assimilation system for seasonal prediction. *Monthly Weather Review*, *139*(3), 786–808. https://doi.org/10.1175/2010mwr3419.1

Yu, L. S., & Weller, R. A. (2007). Objectively analyzed air-sea heat fluxes for the global ice-free oceans (1981–2005). *Bulletin of the American Meteorological Society*, *88*(4), 527–539. https://doi.org/10.1175/BAMS-88-4-527

References From the Supporting Information

Abe, O., Agata, S., Morimoto, M., Abe, M., Yoshimura, K., Hiyama, T., & Yoshida, N. (2009). A 6.5-year continuous record of sea surface salinity and seawater isotopic composition at Harbour of Ishigaki Island, southwest Japan. *Isotopes in Environmental and Health Studies*, *45*(3), 247–258. https://doi.org/10.1080/10256010903083847

Benway, H. M., & Mix, A. C. (2004). Oxygen isotopes, upper-ocean salinity, and precipitation sources in the eastern tropical Pacific. *Earth and Planetary Science Letters*, *224*(3–4), 493–507. https://doi.org/10.1016/j.epsl.2004.05.014

Garcia, A. M., Winemiller, K., Hoeinghaus, D., Claudino, M., Bastos, R., Correa, F., et al. (2017). Hydrologic pulsing promotes spatial connectivity and food web subsidies in a subtropical coastal ecosystem. *Marine Ecology Progress Series*, *567*, 17–28. https://doi.org/10.3354/meps12060

IAEA/WMO. (2022). International atomic energy agency/world meteorological organization global network for isotopes in precipitation. *The GNIP Database*. Retrieved from https://www.iaea.org/services/networks/gnip

Moore, W. S. (1999). The subterranean estuary: A reaction zone of ground water and sea water. *Marine Chemistry*, *65*(1–2), 111–125. https://doi.org/10.1016/s0304-4203(99)00014-6

Morimoto, M., Abe, O., Kayanne, H., Kurita, N., Matsumoto, E., & Yoshida, N. (2002). Salinity records for the 1997-98 El Nino from Western Pacific corals. *Geophysical Research Letters*, *29*(11), 1540. https://doi.org/10.1029/2001GL013521